ARTICLE

ACS chemical biology

Identification of Novel Small Molecule Inhibitors of the XPA Protein Using *in Silico* Based Screening

Tracy M. Neher[†,∥], Sarah C. Shuck[‡,∥], Jing-Yuan Liu[§], Jian-Ting Zhang[§], and John J. Turchi[†,‡,*]

[†]Department of Medicine, [‡]Department of Biochemistry and Molecular Biology, and [§]Department of Pharmacology and Toxicology, Indiana University School of Medicine, Indianapolis, Indiana 46202, [∥]These authors contributed equally to this work.

ABSTRACT The nucleotide excision repair pathway catalyzes the removal of bulky adduct damage from DNA and requires the activity of more than 30 individual proteins and complexes. A diverse array of damage can be recognized and removed by the NER pathway including UV-induced adducts and intrastrand adducts induced by the chemotherapeutic compound cisplatin. The recognition of DNA damage is complex and involves a series of proteins including the xeroderma pigmentosum group A and C proteins and the UV-damage DNA binding protein. The xeroderma pigmentosum group A protein is unique in the sense that it is required for both transcription coupled and global genomic nucleotide excision repair. In addition, xeroderma pigmentosum group A protein is required for the removal of all types of DNA lesions repaired by nucleotide excision repair. Considering its importance in the damage recognition process, the minimal information available on the mechanism of DNA binding, and the potential that inhibition of xeroderma pigmentosum group A protein could enhance the therapeutic efficacy of platinum based anticancer drugs, we sought to identify and characterize small molecule inhibitors of the DNA binding activity of the xeroderma pigmentosum group A protein. *In silico* screening of a virtual small molecule library resulted in the identification of a class of molecules confirmed to inhibit the xeroderma pigmentosum group A protein−DNA interaction. Biochemical analysis of inhibition with varying DNA substrates revealed a common mechanism of xeroderma pigmentosum group A protein DNA binding to single-stranded DNA and cisplatin-damaged DNA.

Xeroderma pigmentosum group A (XPA) is a 31 kDa protein that is required for the nucleotide excision repair pathway (NER), the main pathway mammalian cells use for the repair of bulky DNA adducts (*1*). Inactivating mutations in XPA result in a NER null phenotype and, in humans, the disease xeroderma pigmentosum (XP) (*2*). XPA is a component of the preincision complex involved in the recognition of damaged DNA and has been shown to contain domains that interact with several other proteins in the pathway, including replication protein A (RPA), ERCC1, and XPC-Rad23B (*3*). Once initial damage recognition has occurred, the coordination of several proteins is required for incision and removal of damaged DNA including TFIIH and the XPG and XPF/ERCCI nucleases. Following excision of the damaged strand, the 3′OH resulting from XPF/ERCC1 incision is extended by DNA polymerase δ or ε followed by ligation by DNA ligase I. In addition to ligation by DNA ligase I, an alternative ligation pathway has been demonstrated that employs XRCC1 and DNA ligase III (*4*).

XPA's role in damage recognition has been studied extensively, and it has been shown to interact with both damaged and undamaged DNA (*5, 6*). DNA binding activity has been shown to reside in a 122 amino acid minimal DNA binding domain (MBD) spanning from M98 to F219 that contains a class IV, C4-type zinc-binding motif (*7–9*). A separate study shows that this cleft overlaps with the region for RPA p70 binding as well, supporting the possible cooperative model of DNA binding between XPA and RPA (*10*). The overall structure of the zinc-binding domain varies from those of other zinc finger domains; however, the local four cysteine residues contained in this domain are similar to

*Corresponding author, jturchi@iupui.edu.

Received for review February 24, 2010 and accepted July 27, 2010.

Published online July 27, 2010

10.1021/cb1000444

the zinc fingers found in the GATA-1 transcription factor (*7*). XPA's essential role in NER is a function of DNA interactions and potentially interactions with other NER proteins.

Clinical XP is characterized by an increased predisposition to cancer and extreme sensitivity to UV light (*11*). There are 7 complementation groups, A−G, with XPA being the most severe and having the greatest sensitivity to UV light and other DNA-damaging agents including cisplatin. Consistent with this fundamental role in NER catalyzed repair, increased XPA expression has been associated with decreased sensitivity to DNA-damaging chemotherapeutic agents (*12*). Specifically, increased sensitivity to cisplatin therapy in testicular cancer cells has been linked to decreased levels of XPA, which results in decreased levels of NER activity, and overexpression of XPA in these cells results in a more resistant phenotype (*12*).

Cisplatin is a common chemotherapeutic used in the treatment of several cancers including lung, ovarian, and testicular cancers (*13*). Lung and ovarian cancer patients represent one of the highest mortality rates of all cancer patients diagnosed every year. Currently, cisplatin is a component of the first-line treatment for patients diagnosed with advanced stage non-small cell lung cancer (NSCLC); however, response rates vary and are often short-lived (*14*). However, no other treatments have been shown to be more effective and thus a large majority of these patients will receive cisplatin in the course of their therapy (*15*). Although cisplatin is a front line therapy in the treatment of NSCLC, efficacy varies significantly between patients, causing a spectrum of responses. Differences in the metabolism and uptake of cisplatin as well as the repair of cisplatin−DNA lesions represent a few of the factors thought to influence cisplatin sensitivity (*16, 17*). While a direct correlation of clinical resistance with differential expression of individual NER proteins has not been established, the decreased expression of ERCC1 has been correlated with a better prognosis and response to cisplatin-based therapy following surgery (*18*). Overall these data suggest that by decreasing NER capacity, one could increase sensitivity to cisplatin and potentially approach clinical efficacy observed in testicular cancer response to cisplatin where 95% of patients are cured by a cisplatin based regimen (*13*).

Targeting protein−DNA interactions has only recently been reported in a small number of studies. Peptide-based molecules were used recently to target the sequence specific Notch transcription factor (*19*). Small molecules have also been identified *via* a high-throughput screen (HTS) using fluorescence polarization (FP) as a readout targeting the sequence specific DNA-binding transcription factor HOXA13 (*20*). In addition, we have reported the development of fluorescence-based HTSs to identify SMIs of the damage-specific DNA binding proteins RPA and XPA (*21–23*). In this report we present an *in silico* screen for small molecules that target the DNA binding domain of XPA. A 3-D structure obtained *via* NMR of the XPA minimal DNA binding domain (MBD) reveals a cleft that includes a number of conserved basic amino acids, which using chemical shift perturbation experiments has been suggested to be in direct contact with the DNA in conjunction with surrounding residues (*24*). In addition, Lys141 and 179, found within this cleft, were shown to impact binding to kinked DNA substrates, presumably similar to those formed by bulky DNA adducts that are repaired by NER (*25*). The characteristics of this cleft make it an ideal site for small molecule drug screening with the goal of identifying small molecules that bind to this cleft and disrupt the direct interaction between XPA and DNA and potentially cooperative DNA binding effects between RPA and XPA as this region also interacts with RPA (*10*). In this study, we performed a structure-based *in silico* screen targeting this cleft and identified small molecules capable of inhibiting the XPA−DNA interaction. Characterization of these molecules provides proof-of-concept for targeting a DNA binding activity *via in silico* analysis and reveals similar mechanisms of XPA binding to structurally diverse DNA substrates.

RESULTS AND DISCUSSION

Targeting Nucleotide Excision Repair. The NER pathway is responsible for the removal of a vast array of DNA damage from the human genome including environmental DNA damage such as that caused by exposure to UV light and chemotherapy-induced DNA damage typified by the agent cisplatin (*4, 26*). This pathway requires the concerted activity of over 30 proteins, and despite *in vitro* reconstitution of the pathway over 15 years ago, the fundamental mechanism required for many of the steps remains elusive (*3, 27*). This is no more apparent than in the initial step of DNA damage recognition. The damage recognition step in NER is complicated by the requirement to respond to a wide array of DNA

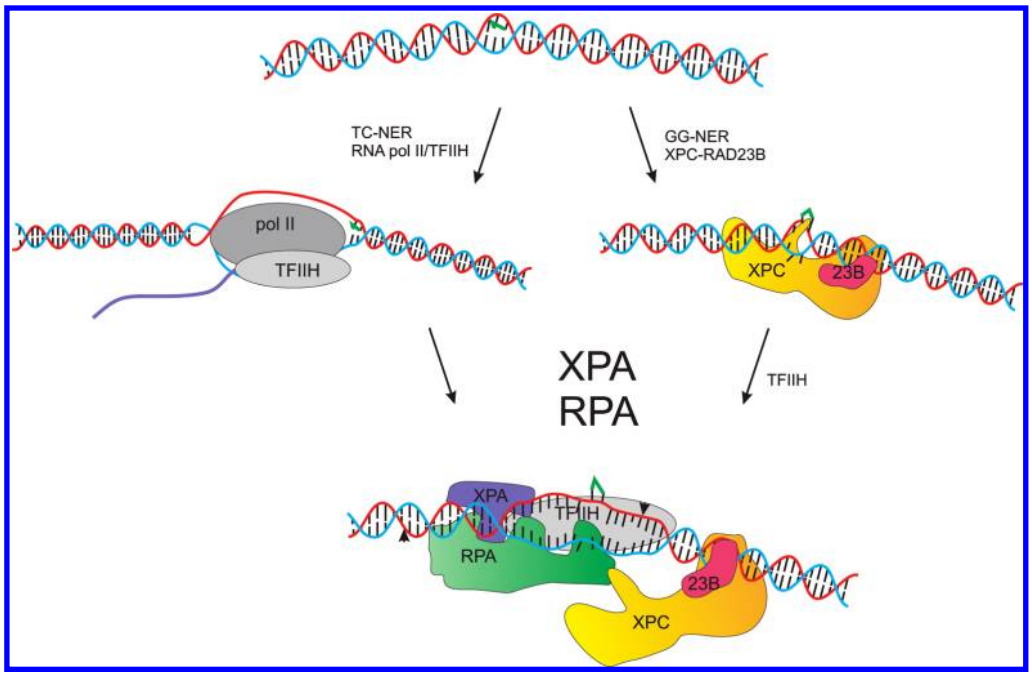

Figure 1. Recognition of DNA damage *via* the NER pathway. Recognition of DNA damage *via* TC-NER proceeds *via* RNA pol II encountering the lesion in complex with TFIIH. The addition of XPA and RPA completes the recognition process. In GG-NER, the XPA-Rad23B complex encounters the damage site followed by XPA-RPA and TFIIH, after which XPC dissociates from the DNA. Following both processes, the structure-specific nucleases XPF-ERCC1 and XPG catalyze incision 5′ and 3′ of the lesion indicated by the arrowheads. The damaged DNA strand is depicted in red, the undamaged strand is in blue, and the cisplatin lesion is in green. The transcribed mRNA is depicted in dark blue.

damage so that unforeseen chemical insults to DNA can be repaired. Thus recognition must rely not on a single chemical modification but on the gross distortion in the DNA structure induced by DNA damage. This issue together with the bifurcation of recognition into two pathways, transcription coupled NER (TC-NER) and global genomic NER (GG-NER), results in a further increase in complexity (Figure 1). The role of the XPA protein in DNA damage recognition is well established though the mechanistic and temporal regulation of how this protein participates in the process remains less well-defined. Considering the importance of XPA in the recognition of cisplatin DNA damage and the demonstration that reducing XPA can sensitize cells to this therapeutic agent raises the possibility that small molecule inhibitors (SMIs) targeting XPA may have therapeutic potential to increase the efficacy of cisplatin-based therapies and reverse resistance that results from efficient repair of cisplatin-induced DNA lesions.

***In Silico* Screening To Identify Small Molecules That Interact with XPA's DNA Binding Domain.** Previous high-throughput assay-based screening of a small molecule library identified a number of compounds with putative inhibitory activity toward the XPA–DNA interaction (*23*). However, verification of this inhibitory activity in secondary screening assays was largely unsuccessful (data not shown). We therefore undertook an *in silico*

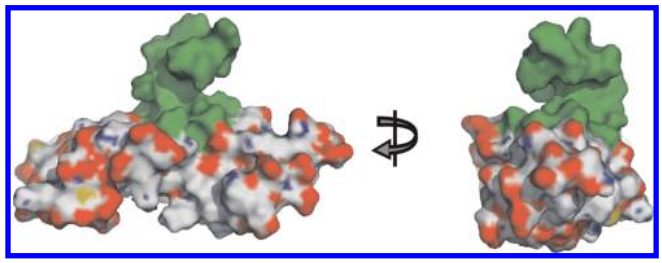

Figure 2. XPA-minimal DNA binding domain. Model of XPA MBD highlighting the region of the protein targeted for *in silico* screening. The targeted cleft is depicted in green, and the image is rotated 90°.

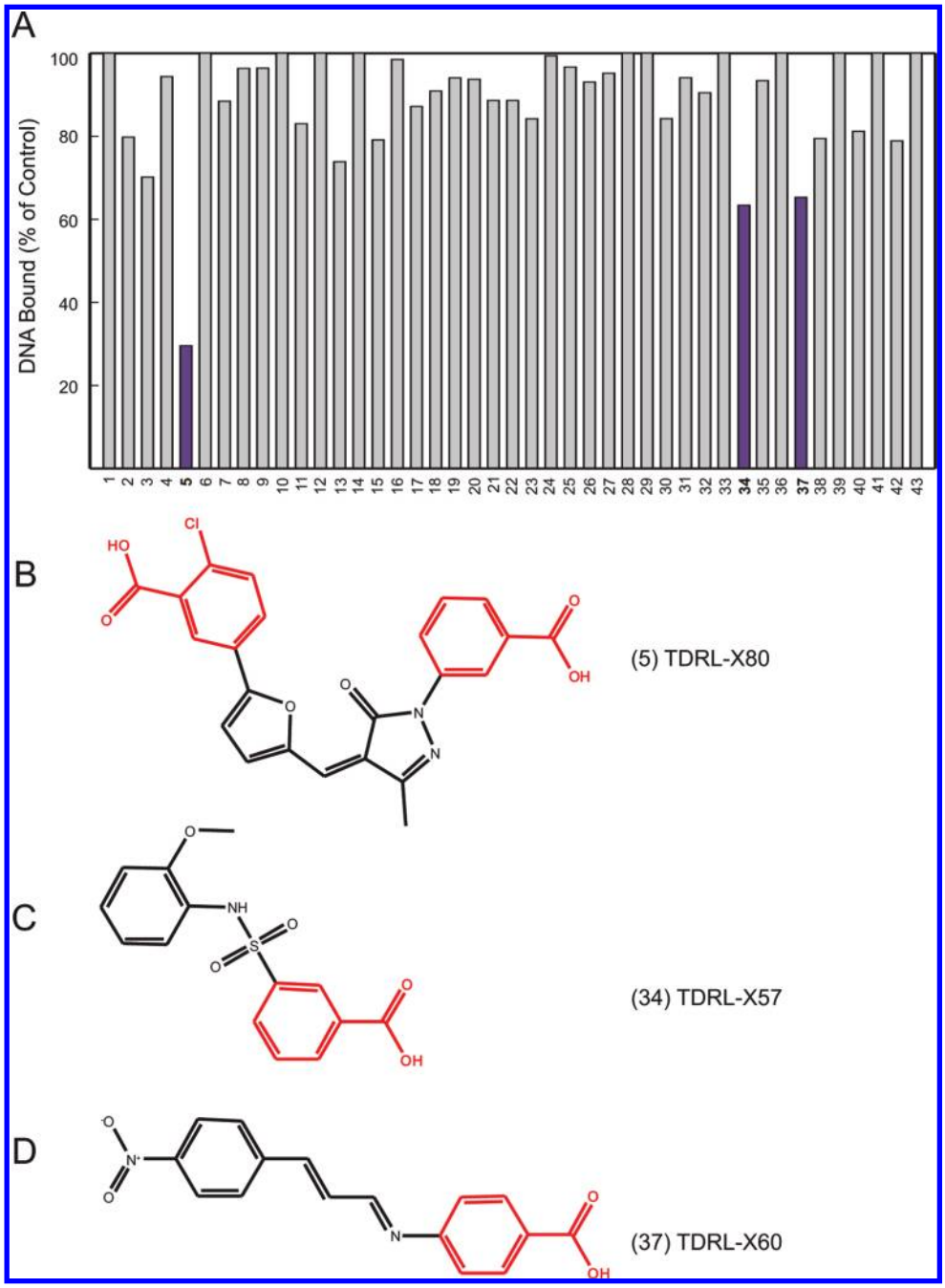

Figure 3. *In vitro* analysis and chemical structures of XPA inhibitors. A) Analysis of *in vitro* inhibitory activity against XPA–DNA binding of compounds identified from the *in silico* screen by fluorescence polarization was performed as described in Methods. B–D) Chemical structures of SMIs identified in the *in silico* screen are depicted with the common structural features colored red.

screening approach toward the discovery of novel compounds that can interact with XPA and hold the potential to inhibit the DNA binding function of XPA. Using the 3D structure of XPA determined by NMR (PDB code

1XPA), the coordinates of the C-terminal subdomain (residues 131−210) that have been shown to be in direct contact with a DNA ligand were employed in the *in silico* analysis. The cleft consisting of residues 138−142, 165−171, 174, and 177−181 was chosen as the targeted area for small molecule docking (Figure 2). The ChemDiv virtual library was screened as described in Methods, and 63 putative inhibitors of XPA's DNA binding activity were identified and subjected to a secondary *in vitro* activity analysis to directly test their ability to interact with XPA and inhibit the XPA−DNA interaction. FP analysis using purified XPA (*28*) and a fluorescein-labeled single-strand DNA substrate was performed. Of the 63 compounds identified in the *in silico* screen, 3 were found to inhibit XPA's DNA binding activity *in vitro* (Figure 3, panel A) (*23, 29*). Each of the compounds with verified *in vitro* activity contain a benzoic acid substituent and in the case of X80, two such moieties at either end of the molecule (Figure 3, panel B). Compound X57 contains a methoxybenzene substituent with a sulfomyl separating the benzoic acid (Figure 3, panel C). Compound X60 contains a nitrobenzene distal to the benzoic acid bridged by an unsaturated amine spacer (Figure 3, panel D). Interestingly, compounds identified in the original HTS did not share any structural characteristics with the SMIs identified by the *in silico* screen and confirmed by *in vitro* analysis. For example, SMIs X80, 57, and 60 all contain at least one acidic moiety, whereas compounds identified by the HTS in general lacked this functional group. This data demonstrate the utility of *in silico* screening to identify SMIs of XPA.

***In Vitro* Characterization of Putative XPA Inhibitors: Fluorescence Polarization and DNA Substrate Specificity.** *In silico* analysis identified compounds that putatively interact with XPA's DNA binding domain; however, preliminary *in vitro* FP analyses were used to confirm the interaction of each compound with XPA and inhibition of DNA binding activity. We therefore extended these FP studies to assess potency and specificity for different DNA substrates to which XPA has been shown to bind. We employed single-strand DNA and fully duplex DNA that was either undamaged or contained a single site specific cisplatin 1,2 d(GpG) adduct centrally located in the duplex. Each of these substrates was prepared with a 5′-fluorescein label, and XPA was titrated with each DNA substrate to determine the concentration required to bind 70% of the input DNA. Each compound was then titrated from 0 to 100 μM with a fixed concentration of XPA to determine if the compound inhibited XPA's DNA binding activity. The data presented in Figure 4 measuring binding to the single-stranded DNA substrate reveal that X80 displays the greatest in-

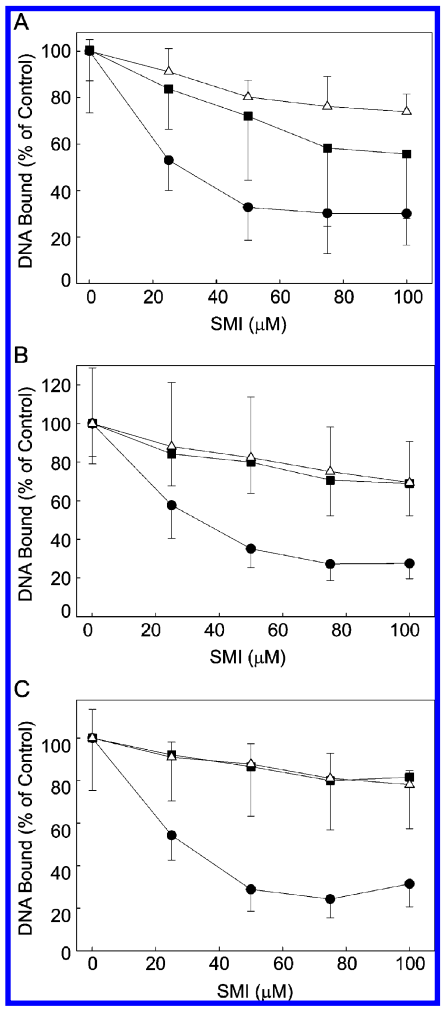

Figure 4. XPA inhibitors reduce XPA−DNA complex formation *in vitro*. X80 (●), X57 (■), and X60 (△) were added in increasing concentrations to fluorescein-labeled single-strand DNA (A), cisplatin-damaged duplex DNA (B), and undamaged duplex DNA (C). Fluorescence polarization was monitored, and DNA binding was determined as described in Methods. The data are presented as the reduction in DNA binding compared to an untreated control and represent the mean and SD from three independent experiments.

TABLE 1. Calculated IC_{50} values for TDRL-X80 on single, double, and cisplatin-damaged DNA as determined by fluorescence polarization and ELISA analysis[a]

	IC_{50} values (μM)	
DNA substrate	Fluorescence polarization	ELISA
single strand	18 ± 11	21 ± 3
ds-unplatinated	20 ± 10	39 ± 14
ds-platinated	29 ± 16	28 ± 8

[a]Inhibition values were obtained as described in Methods.

hibitory activity, whereas both X57 and X60 show less inhibition (panel A). The same trend is also evident in the analysis of XPA binding to duplex undamaged DNA and a duplex DNA containing a single 1,2 d(GpG) cisplatin−DNA adduct (panels B and C, respectively). The data were quantified for compound X80 on the three different substrates, and IC_{50} values were calculated using a 3-parameter hyperbolic decay with offset (Table 1). There was no statistical differences observed in the calculated IC_{50} values, which suggests a common mode of XPA binding to each DNA substrate that was equally inhibited by X80. IC_{50} values for compounds X57 and X60 were not calculated because the compounds never resulted in inhibition of XPA's DNA binding ability by more than 50%, indicating a weaker interaction with XPA compared to that of X80. Although FP is a highly accurate and quantitative assay for DNA binding, the potential for interference as a result of spectroscopic properties of the compounds led us to assess the effect of these three inhibitors in a nonspectroscopic assay.

***In Vitro* Inhibition of XPA's DNA Binding Activity As Determined by Modified ELISA Assay.** In order to confirm the *in vitro* activity of the three lead small molecule inhibitors, an ELISA assay was used to assess the ability of these compounds to prevent XPA from binding DNA. In this assay, biotin-conjugated 60-base single-strand DNA was bound to streptavadin-coated ELISA plates. Purified XPA was titrated into the binding reactions to determine the concentration that resulted in approximately 50% XPA DNA binding activity, which was determined to be 10 ng of protein (data not shown). XPA was then preincubated with either vehicle or compound and then added to the wells containing the biotin conjugated DNA. Following incubation, the plates were washed, and bound XPA was detected using an anti-XPA polyclonal antibody followed by an HRP conjugated goat antirabbit IgG secondary antibody. HRP activity was determined kinetically using a TMB-based substrate as described in Methods. Initial analyses at relatively high concentrations revealed that at concentrations up to 200 μM, no inhibition of binding was observed with compounds X57 and X60 (Figure 5, panel A), whereas X80 inhibited XPA binding by 95% at a concentration of 100 μM. The ELISA assay requires a greater affinity to detect an interaction than the FP assay. The complex must be stable during the washing and probing steps, and thus it is not a true equilibrium binding assay. However, the analyses do give an accurate measure of the portion of XPA that is capable of binding the immobilized substrate. That X57 and X60 do not display inhibitory activity in this assay is consistent with low inhibitory activity observed in the FP assay. Confirmatory analysis of the inhibitory activities of these compounds was obtained using a photo-cross-linking approach as we described previously in the analysis of XPC-Rad23B binding to cisplatin-damaged DNA (*30*). Binding of XPA to a duplex DNA substrate containing a single cisplatin 1,2 d(GpG) adduct modified with a single photoactivateable dCTP 5′ of the lesion was assessed. Increasing concentrations of each inhibitor was included, and the DNA−protein complexes cross-linked and products were resolved by SDS -PAGE and visualized by phosphorimager analysis. The data confirm inhibitory activity of X80 with only less inhibition observed for X57 and X60 (Supplementary Figure S1).

On the basis of this analysis, X57 and X60 were not analyzed further for *in vitro* activity, and X80 was assessed on each of the substrates, single-stranded DNA, duplex undamaged DNA, and a 1,2 (GpG) cisplatin-damaged duplex DNA (Figure 5). These data demonstrate that X80 again displayed similar inhibitory activity when comparing inhibition of XPA on the single-strand, duplex-damaged DNA and undamaged duplex DNA substrates (Figure 5, panels C and D). The calculated IC_{50} values (Table 1) did not reveal a significant difference among the DNA substrates. This result is again consistent with the FP data and indicates that the compound is interacting with XPA in a way that prevents its binding to various types of DNA substrates. The close concordance between the two independent assays sug-

gests that the interaction of X80 with XPA disrupts the ability of XPA to bind to each of the DNA substrates tested and that the mechanism of XPA binding to each DNA substrate is similar.

Considering the relatively high concentrations necessary to inhibit XPA, the potential for aggregation of the compound inducing nonspecific inhibition can be a concern. High speed centrifugation of the compound did not, however, result in precipitation of the compound (data not shown) thus ruling out the possibility that gross aggregation or the presence of a precipitate is responsible for inhibition of XPA. While insoluble aggregation was ruled out, soluble aggregation has also been reported for some chemical compounds identified from *in vitro* HTS (*31–33*). Importantly, both the FP- and ELISA-based DNA binding assays are performed in a buffer that contains a low level of nonionic detergent (0.01% NP40) to disrupt potential aggregation of the small molecules. The use of these conditions ensures that any inhibition observed was not the result of soluble aggregation (*34*). In addition, analysis of the shape of the inhibition curves is not consistent with aggregation of the compounds, which would be expected to yield a considerable steeper hill slope of inhibition over a smaller concentration range (*33*).

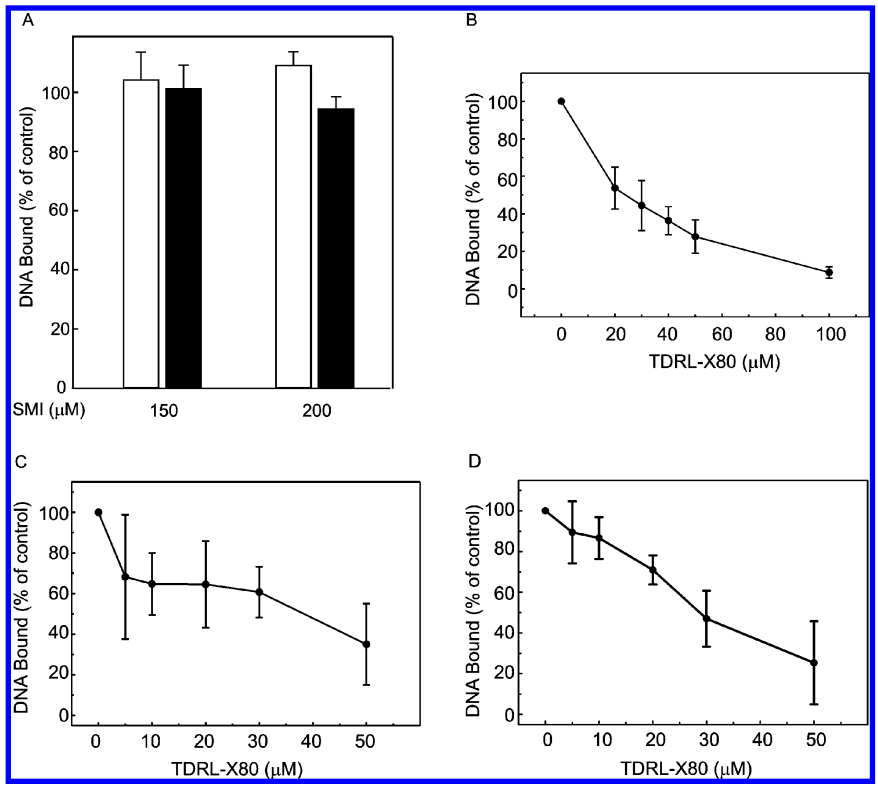

Figure 5. X57 and X60 do not inhibit XPA—DNA binding as assessed in a modified ELISA. The indicated concentrations of X57 (white bars) and X60 (black bars) were incubated with 10 ng of XPA for 10 min and binding to single-strand DNA was assessed by a modified ELISA as described in Methods (A). X80 was preincubated with 10 ng of XPA and analyzed for binding to single-strand DNA (B). XPA (50 ng) was analyzed for binding to undamaged duplex DNA (C), and 10 ng was used for analysis of binding to a duplex DNA containing a single 1,2-dGpG cisplatin lesion (D). The mean percentage of XPA bound compared to DMSO control and SD from at least 3 independent experiments are presented.

Interrogation of SMI Interactions with XPA. To assess the validity and accuracy of the *in silico* screening and docking analysis, additional compounds in the X80 class were obtained from the ChemDiv Library and assessed for XPA inhibition. The derivatives contained modified moieties in place of the substituent on each phenyl ring of X80, providing insight into the importance of the acidic groups. Compound X801 replaces the furanyl 2-chlorobenzoic acid with a 3-chlorophenyl, whereas compound X802 replaces the pyrazole 3-carboxyphenyl in parent X80 compound with a 3-bromophenyl. Both of these modifications resulted in a significant decrease in XPA inhibitory activity with IC_{50} values greater than 0.1 mM as assessed in the ELISA assay (Table 2). That X80 is more active than these two derivatives provides support for the accuracy of the *in silico* screen as the derivatives; X801 and X802 were ranked lower on the basis of binding characteristics and ΔG values compared to those of X80. These data also demonstrate that each of the acidic functional groups is critical to XPA inhibitory function. The third derivative investigated replaced the furanyl 2-chlorobenzoic acid with a 2- hydroxy-5-nitrophenyl. This compound exhibited intermediate inhibitory activity with an IC_{50} of approximately 75 μM, consistent with the importance of a negatively charged or acidic functional group (Table 2) and again providing further support for the *in silico* screen and selection process. Importantly, minor changes in substitutions on the furan benzene including removal of the *p*-Cl or replacing the carboxyl with an ester moiety resulted in in-

TABLE 2. *In vitro* analysis of activity of X80 derivatives on XPA–DNA binding[a]

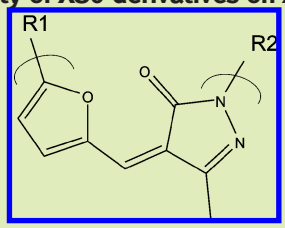

TDRL-	R1	R2	IC_{50} [a]
X801	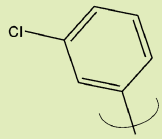	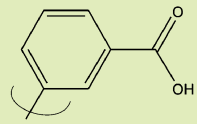	>100 μM
X802	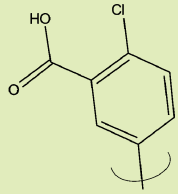	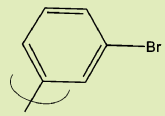	>100 μM
X803	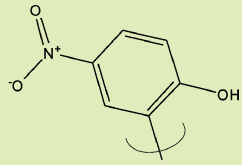	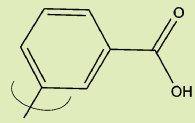	75 μM

[a]Inhibition values were obtained using the modified ELISA assay on a single-stranded 60 based DNA.

hibitory activity very similar to that of the parental X80 compound.

To further investigate the impact of chemical structure on XPA inhibitory activity, we first analyzed component molecules in the X80 structure. Both the 3-(3-methyl-5-oxo-4,5-dihydro-1*H*-pyrazol-1-yl)benzoic acid and 2-chloro-5-(5-formylfuran-2-yl)benzoic acid displayed no inhibitory activity as expected (data not shown). Considering the relative importance of the benzoic acid moieties, we identified small molecules with similar terminal functional groups tethered by a different core structure. Compounds X055 and X126 each contain a modified phenyl bridged by a thiazolidin core structure. The data presented in Figure 6 demonstrate that X055, which contains a 2-bromo-1-methoxybenzene moiety, displays significantly greater activity against XPA compared to X126, which contains a 2-(2-chloro-6-methoxyphenoxy)acetic acid substituent. That the X055 displays a greater affinity for XPA (IC_{50} < 20 μM) than X80 yet has only a single benzoic acid suggests modification to reduce overall negative charge may be possible to allow cellular uptake and activity *in vivo*.

Specificity and Interactions of XPA Inhibitors. To assess specificity, X80 was assessed for inhibitory activity against RPA, a protein with both single-stranded DNA binding and duplex damaged DNA binding activity. No inhibition was observed at 50 μM as assessed in an EMSA-based assay (Supplementary Figure S2). Interestingly, analysis of the effect of X80 on the activity of another DNA binding protein, Ku, did reveal inhibition at 50 μM (Supplementary Figure S2). While inhibition of binding was observed, a more extensive analysis of a series of small molecules containing acidic functional

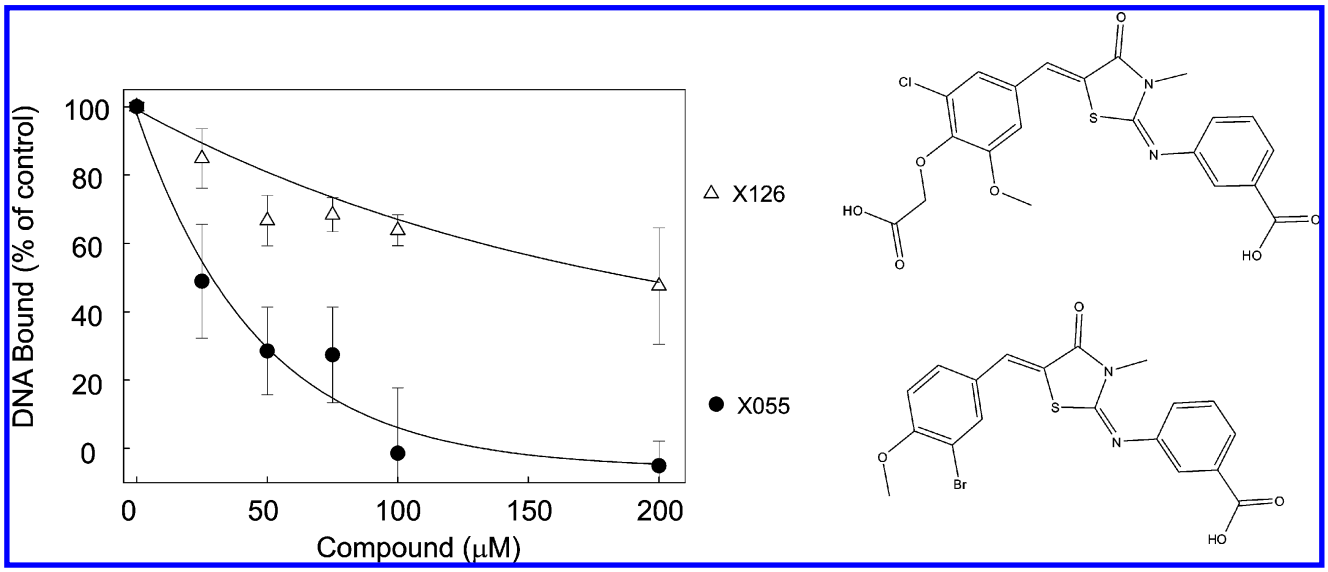

Figure 6. Variable core structure supports XPA inhibition. XPA inhibitor activity of X126 and X056 were assessed by FP analysis using a single-strand DNA substrate. Fluorescence polarization was monitored and DNA binding was determined as described in Methods. The data are presented as the reduction in DNA binding compared to an untreated control and represent the mean and SD from three independent experiments. Chemical structures of the two inhibitors are presented.

groups with varying core structures revealed inhibition of Ku-DNA binding activity. This result is potentially a function of Ku's unique mode of binding DNA, which involves entry from a terminus and sliding along the duplex DNA. The channel in which DNA threads is populated with a large number of basic residues that interact with the sugar−phosphate backbone of DNA and the potential ionic interactions with benzoic acid groups may impede entry of the DNA into this cavity (*35*).

An alternative explanation for the inhibitory data is that the X80 compound is interacting with DNA, making it unable to bind to the proteins. Although the chemical structure, with the presence of two negatively charged carboxyl groups, would suggest this is unlikely, we analyzed this interaction directly using a fluorescent intercalator dye displacement assay (*36*). The results demonstrate that the compound alters the fluorescence only at concentrations greater than 100 μM, which is attributed to the spectral properties of the compound quenching the signal (data not shown). This demonstrates that the X80 compound is not imparting its inhibitory activity *via* interacting with the DNA, and therefore the reduction of an XPA−DNA complex in the presence of X80 is due to a direct X80−XPA interaction.

Molecular Modeling of the Putative Interactions within the XPA MBD. As there are two known XPA structures with different conformations in loop 2, which has been shown to be directly involved in ligand binding, we next examined how X80 would interact with the two different structures by docking analysis (Figure 7, panels A and B). The best X80 conformation docked into the 1D4U (panel B) XPA structure had an orientation and conformation similar to that in the 1XPA structure (panel A). The grid scores of X80 in the two structures are also similar with −47 and −43 kcal mol^{-1}, respectively (Table 3). We also analyzed X57 and X60 by docking into both XPA structures. As shown in Table 3, both X57 and X60 similarly did not score well in either structure. These data are completely consistent with the *in vitro* DNA binding data showing minimal inhibitory activity of X57 and X60. In addition, the difference in loop 2 conformations of the two structures does not significantly affect the calculated binding affinity of these ligands.

To gain further insight into the potential interactions between XPA and the SMIs, the data obtained from the *in silico* docking was analyzed. Inspection of the position of X57 and X60 reveal potential salt bridges between the benzoic acid carboxyl of each compound and

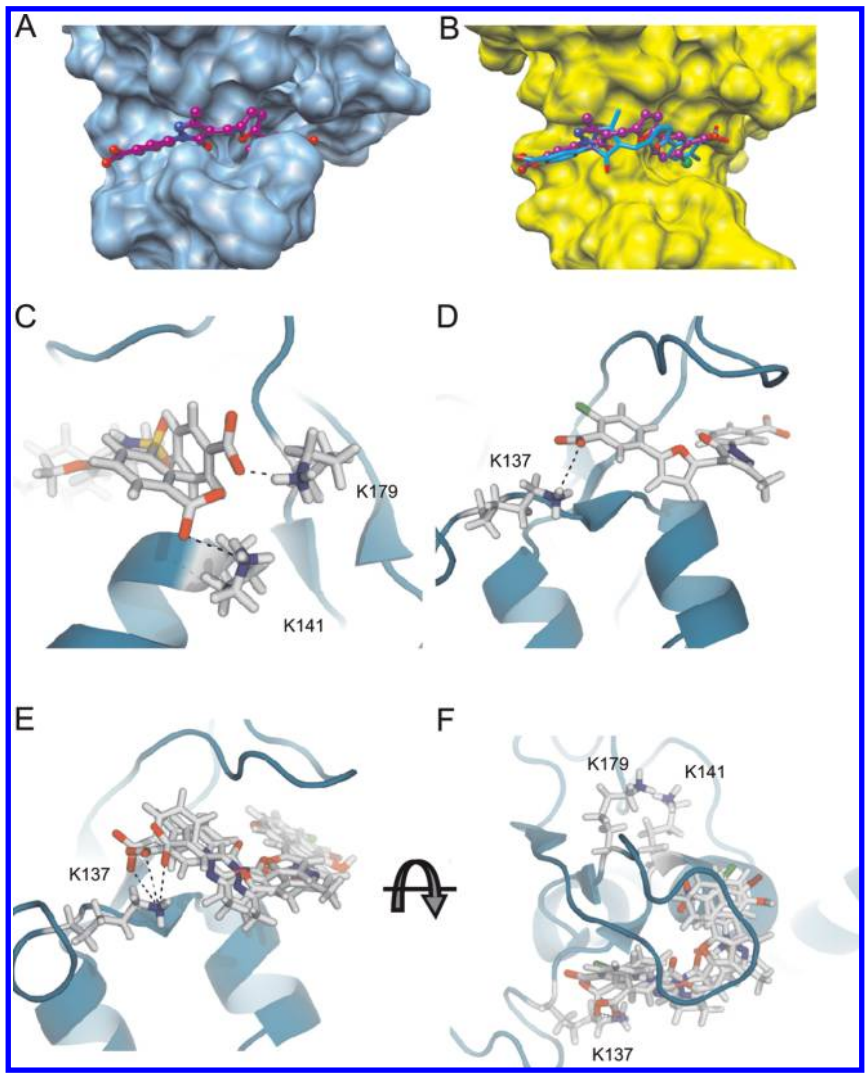

Figure 7. Docking analysis of SMI interactions with XPA. The docked X80 orientation and conformation in two XPA structures. A) X80 in 1XPA is shown in purple in ball-and-stick representation. B) X80 docked in the 1D4U structure with best score shown in blue in stick representation. The X80 orientation and conformation in 1XPA is also shown in 1D4U (purple) for comparison. C) Modeling X57 and X60 in the 1XPA MBD. Lys141 and 179 are within interacting distance to the benzoic acid from each compound. D) Docking results with X80 reveals interactions of the furanyl benzoic acid with Lys137. E) Analysis of X801, X802, and X803, which each contain a single benzoic acid, reorient within the MBD cleft to maintain an interaction with Lys137. F) Rotation of panel C by 90°.

Lys141 and 179 (Figure 7, panel C). Interestingly, docking of X80, the most active inhibitor, positioned the carboxyl outside the range of electrostatic interaction but did reveal the potential for hydrogen bonds with Thr142 or Ser173. Of the three compounds, X80 was extended further through the cleft and positioned the furanyl benzoic acid carboxyl group in range for interactions with Lys137 (Figure 7, panel D). Confirmation of the importance of this interaction was obtained by inspection of the docking results with compounds X801, X802, and X803. In X802, the carboxyl functional group of the pyrole benzene was replaced with a halogen. Docking results revealed a very similar overall position of the furnayl and pyrole ring systems, and the remaining benzoic acid carboxyl group retained the ionic interaction with Lys137. Surprisingly, docking analysis of compounds X801 and X803, in which the furan benzoic acid is replaced with either a halogen- or nitro-substituted benzene, results in reorientation of the compounds within the XPA DNA binding domain to retain the Lys137 interaction with the remaining benzoic acid carboxyl (Figure 7, panels E and F). These data support the conclusion that each benzoic acid in the parent X80 compound is stabilized *via* interactions with basic amino acids and that the Lys137 salt bridge is a critical determinant of inhibitory activity. Interestingly, analysis of XPA structure and function demonstrated that individual mutations of Lys141 or 179 to alanine or glutamine had minimal influence on NER activity and XPA–DNA binding; however, a double K141E/K179E mutation displayed reduced repair and XPA–DNA binding to linear duplex DNA substrates (*25*). That such a dramatic alteration in ionic character is required for abrogation of activity suggests there are overlapping redundant binding sites within the XPA DNA binding domain. This is further supported by demonstration that the double mutant is fully capable of binding 4-way junction, severely kinked DNA (*25*). Our chemical inhibition data further suggest a larger binding domain with additional points of contact that extends beyond the cleft to encompass Lys137. An alternative and somewhat less likely possibility is that positioning of X80 through the cleft contacting Lys137 induces a conformational change that abrogates DNA binding at a separate site. In light of these analyses it would be of considerable interest to determine if Lys137 is required for DNA binding and/or to potentiate the inhibitory activity

TABLE 3. Docked grid scores in 1XPA and 1D4U conformation

	Docking grid score (kcal mol^{-1})	
TDRL	1XPA	1D4U
X57	−37	−36
X60	−37	−34
X80	−47	−43

of X80. It is important to note that these docking studies represent models for potential interactions between XPA MBD and the SMIs. Our *in vitro* analyses were all performed with full length XPA, and we cannot rule out that the inhibitors interact with other sites in XPA that potentially influence DNA binding activity. Definitive proof of the site of X80 binding and specific interactions will require high-resolution structural analyses.

We would anticipate that the ability to inhibit XPA *in vivo* would be of significant utility from a variety of perspectives. Importantly, *in vivo* inhibition of XPA would be expected to result in decreased repair of bulky adduct DNA damage *via* NER. This has potential as a therapeutic strategy in the treatment of cancer in conjunction with DNA-damaging chemotherapeutics including cisplatin that are repaired *via* NER. As alterations in DNA repair have been suggested to play an important and potentially targetable pathway (*37*), the identification of SMIs capable of disrupting this process could be extremely useful. This is currently being observed in the clinical treatment of cancer with inhibitors of the poly-ADP ribose polymerase (*38*). Although the exact mechanisms involved in the therapeutic activity remain to be determined, the clinical activity can be dramatic, and thus identifying new targets and agents to build upon these successes holds great promise.

METHODS

Structure-Based *in Silico* Screening. In order to identify small molecules that can disrupt the XPA−DNA interaction, we first examined the solution NMR structures of the central domain of XPA (PDB ID codes 1XPA (*39*) and 1D4U (*40*)). The loop 2 (residues 166−179), which has been shown to be directly involved in DNA binding, appears to have very different conformations in these two structures with a RMSD of 6.1 Å for CA atoms. Comparison of these two structures showed that the putative DNA binding groove in the 1XPA structure is narrower and deeper with a more closed conformation. The difference between these two structures may explain the flexibility of XPA in recognizing a wide variety of DNA lesions. The more closed and deep groove of 1XPA makes it more suitable for performing docking experiments. Consequently, the central domain of the 1XPA structure was used for *in silico* screening.

The molecular surface of the central domain of XPA was calculated by the DMS program. Partial charges and protons were added to the protein by UCSF Chimera Dock Prep module (*41*). The small molecules used in the virtual screening are from the ChemDiv library, in which the 3D models were converted from the 2D chemical structures provided by ChemDiv catalogs using SYBYL6. More than 200,000 compounds were docked and screened to the cleft by UCSF DOCK 6 program (*42*). Compounds were first scored with the DOCK GRID scoring function (*43*), following which the top 2,000 compounds were rescored by AMBER score function incorporated in DOCK 6 (*44*). The top 1,000 compounds were then clustered by MOE, and the docked compounds were visually examined using the UCSF Chimera ViewDock function. Approximately 100 compounds were identified on the basis of GRID and AMBER scores, drug likeness (Lipinski's Rule of Five), visual examination of the docked protein−compound complexes, and with consideration of maximizing compounds from different clusters.

Chemicals. Compounds identified were purchased from ChemDiv or SPEX and prepared at 10 mM in 100% DMSO. Confirmation of the structure and purity of TDRL-X80 was determined by LCMS analysis.

Overexpression and Purification of Human [His]$_6$-XPA. [His]$_6$-XPA was purified as previously described (*28*). Briefly, Sf9 cells were infected with XPA virus, and the cellular pellet was lysed by dounce homogenization in buffer A containing 50 mM Tris, 100 mM NaCl, 0.1% (v/v) Triton X-100, 10% (v/v) glycerol, and 10 mM BME, along with a protease inhibitor cocktail. Following sonication, imidazole was added to 1 mM to the cellular extract, which was then loaded onto a 2 mL nickel-NTA agarose column. Bound protein was eluted in buffer A with 80 mM imidazole and protein containing fractions identified using Bradford analysis. Protein containing fractions were then pooled and loaded directly onto a 2 mL heparin-Sepharose column. Protein was eluted using a gradient from 100 mM to 1 M NaCl in heparin buffer (50 mM Tris, pH 7.5, 1 mM EDTA, 10% (v/v) glycerol, and 1 mM DTT with protease inhibitor mix). Fractions containing XPA were identified using Bradford and SDS-PAGE analysis, pooled and dialyzed overnight in heparin buffer and stored at −80 °C.

Fluorescence Polarization. Fluorescence polarization was performed on 30-mer single-strand DNA and duplex DNA with or without a 1,2 d(GpG) cisplatin lesion (10 nM) in buffer containing 20 mM HEPES, 1 mM DTT, 0.01% (v/v) NP40, and 100 mM NaCl. An excitation wavelength of 495 nm and a slit width of 5 nm were used in addition to an emission wavelength of 535 and 10 nm slit width. An XPA concentration of 30 nM (ssDNA) or 250 nM (dsDNA) was used to result in ~70% binding of XPA to DNA. Putative XPA inhibitors were titrated (0−100 μM) and polarizations values read. Results are presented as the average and standard deviation of at least three independent experiments.

ELISA. ELISA assays were performed by binding 200 fmol per well of biotinylated 60 base pair single-strand DNA in blocking buffer (2% (v/v) BSA TBS-Tween) overnight on strepavadin coated plates (Roche Applied Science). Inhibition of protein

binding was examined by incubating 10 ng of purified XPA with increasing concentrations of compound in 150 μL reactions containing 5% (v/v) DMSO and blocking buffer for 10 min at RT. Following incubation, 100 μL of each reaction was added to separate wells, in duplicate, and incubated for 1 h. The amount of XPA bound to DNA was analyzed by incubating 50 μL of goat anti-XPA antibody (Santa Cruz Biotechnology) (1:1000 in blocking buffer) in each well for 30 min with rocking. Following incubation with primary antibody, wells were washed 3 × 5 min with blocking buffer followed by the addition of goat antirabbit secondary antibody (Biorad) (1:2500 in blocking buffer) for 30 min. Wells were then washed as described above and TMB-ELISA reagent (Thermo Scientific) was added to each well. Kinetic reads were performed using a SpectraMax M5 spectrophotometer (Molecular Devices) for 20 min at 30 s intervals at wavelengths 490 and 370 nm. The maximum Abs sec^{-1} absorbance value was determined for each sample and represented as a percentage of the absorbance value obtained for the control treated sample. The averages represent the results of duplicate samples from 4 independent experiments. The IC_{50} and standard deviation were calculated by fitting the curve to a standard 2-parameter hyperbolic curve. ELISA assays for the cisplatin-damaged and undamaged double strand substrates were performed as described above, however, 10 and 50 ng of XPA were used, respectively.

Molecular Modeling of XPA with Small Molecules. XPA interactions with small molecules were viewed using Pymol (DeLano Scientific) using cartoon and surface interaction views. Potential amino acid interactions were determined based on proximity to each compound as revealed by docking analysis.

Acknowledgment: This research was supported with funding from the National Institutes of Health to J.-T.Z. (CA94961) and J.J.T. (CA082741). The authors thank Dr. O. Lavrik for supplying the FAP-dCTP analogue.

Supporting Information Available: This material is available free of charge via the Internet at http://pubs.acs.org.

REFERENCES

1. Asahina, H., Kuraoka, I., Shirakawa, M., Morita, E. H., Miura, N., Miyamoto, I., Ohtsuka, E., Okada, Y., and Tanaka, K. (1994) The XPA protein is a zinc metalloprotein with an ability to recognize various kinds of DNA damage, *Mutat. Res., DNA Repair 315*, 229–237.
2. Jones, C. J., Cleaver, J. E., and Wood, R. D. (1992) Repair of damaged DNA by extracts from a xeroderma pigmentosum complementation group A revertant and expression of a protein absent in its parental cell line, *Nucleic Acids Res. 20*, 991–995.
3. Mu, D., Park, C. H., Matsunaga, T., Hsu, D. S., Reardon, J. T., and Sancar, A. (1995) Reconstitution of human DNA repair excision nuclease in a highly defined system, *J. Biol. Chem. 270*, 2415–2418.
4. Fousteri, M., and Mullenders, L. H. (2008) Transcription-coupled nucleotide excision repair in mammalian cells: molecular mechanisms and biological effects, *Cell Res. 18*, 73–84.
5. Hermanson-Miller, I. L., and Turchi, J. J. (2002) Strand-specific binding of RPA and XPA to damaged duplex DNA, *Biochemistry 41*, 2402–2408.
6. Camenisch, U., Dip, R., Vitanescu, M., and Naegeli, H. (2007) Xeroderma pigmentosum complementation group A protein is driven to nucleotide excision repair sites by the electrostatic potential of distorted DNA, *DNA Repair (Amst) 6*, 1819–1828.
7. Buchko, G. W., Ni, S., Thrall, B. D., and Kennedy, M. A. (1998) Structural features of the minimal DNA binding domain (M98-F219) of human nucleotide excision repair protein XPA, *Nucleic Acids Res. 26*, 2779–2788.
8. Hess, N. J., Buchko, G. W., Conradson, S. D., Espinosa, F. J., Ni, S., Thrall, B. D., and Kennedy, M. A. (1998) Human nucleotide excision repair protein XPA: extended X-ray absorption fine-structure evidence for a metal-binding domain, *Protein Sci. 7*, 1970–1975.
9. Buchko, G. W., and Kennedy, M. A. (1997) Human nucleotide excision repair protein XPA: ^{1}H NMR and CD solution studies of a synthetic peptide fragment corresponding to the zinc-binding domain (101−141), *J. Biomol. Struct. Dyn. 14*, 677–690.
10. Daughdrill, G. W., Buchko, G. W., Botuyan, M. V., Arrowsmith, C., Wold, M. S., Kennedy, M. A., and Lowry, D. F. (2003) Chemical shift changes provide evidence for overlapping single- stranded DNA- and XPA-binding sites on the 70 kDa subunit of human replication protein A, *Nucleic Acids Res. 31*, 4176–4183.
11. Stary, A., and Sarasin, A. (2002) The genetics of the hereditary xeroderma pigmentosum syndrome, *Biochimie 84*, 49–60.
12. Koberle, B., Masters, J. R. W., Hartley, J. A., and Wood, R. D. (1999) Defective repair of cisplatin-induced DNA damage caused by reduced XPA protein in testicular germ cell tumours, *Curr. Biol. 9*, 273–276.
13. Einhorn, L. H. (2002) Curing metastatic testicular cancer, *Proc. Natl. Acad. Sci. U.S.A. 99*, 4592–4595.
14. Schiller, J. H., Harrington, D., Belani, C. P., Langer, C., Sandler, A., Krook, J., Zhu, J., and Johnson, D. H. (2002) Comparison of four chemotherapy regimens for advanced non-small-cell lung cancer, *N. Engl. J. Med. 346*, 92–98.
15. Bordoni, R. (2008) Consensus conference: multimodality management of early- and intermediate-stage non-small cell lung cancer, *Oncologist 13*, 945–953.
16. Wang, D., and Lippard, S. J. (2005) Cellular processing of platinum anticancer drugs, *Nat. Rev. Drug Discovery 4*, 307–320.
17. Siddik, Z. H. (2003) Cisplatin: mode of cytotoxic action and molecular basis of resistance, *Oncogene 22*, 7265–7279.
18. Zheng, Z., Chen, T., Li, X., Haura, E., Sharma, A., and Bepler, G. (2007) DNA synthesis and repair genes RRM1 and ERCC1 in lung cancer, *N. Engl. J. Med. 356*, 800–808.
19. Moellering, R. E., Cornejo, M., Davis, T. N., Del, B. C., Aster, J. C., Blacklow, S. C., Kung, A. L., Gilliland, D. G., Verdine, G. L., and Bradner, J. E. (2009) Direct inhibition of the NOTCH transcription factor complex, *Nature 462*, 182–188.
20. Ng, P. Y., Tang, Y., Knosp, W. M., Stadler, H. S., and Shaw, J. T. (2007) Synthesis of diverse lactam carboxamides leading to the discovery of a new transcription-factor inhibitor, *Angew. Chem., Int. Ed. 46*, 5352–5355.
21. Shuck, S. C., and Turchi, J. J. (2010) Targeted inhibition of Replication Protein A reveals cytotoxic activity, synergy with chemotherapeutic DNA-damaging agents, and insight into cellular function, *Cancer Res. 70*, 3189–3198.
22. Andrews, B. J., and Turchi, J. J. (2004) Development of a high-throughput screen for inhibitors of replication protein A and its role in nucleotide excision repair, *Mol. Cancer Ther. 3*, 385–391.
23. Turchi, J. J., Shuck, S. C., Short, E. A., Andrews, B. J. (2009) Targeting nucletode excision repair as a mechanism to increase cisplatain efficacy, in *Platinum and Other Heavy Metal Compounds in Cancer Chemotherapy* (Bonetti, A., Leone, R., Muggia, F. M., and Howell, S. B., Eds.) pp 177−188, Humana Press, New York.
24. Buchko, G. W., Tung, C. S., McAteer, K., Isern, N. G., Spicer, L. D., and Kennedy, M. A. (2001) DNA-XPA interactions: a (31)P NMR and molecular modeling study of dCCAATAACC association with the minimal DNA-binding domain (M98-F219) of the nucleotide excision repair protein XPA, *Nucleic Acids Res. 29*, 2635–2643.
25. Camenisch, U., Dip, R., Schumacher, S. B., Schuler, B., and Naegeli, H. (2006) Recognition of helical kinks by xeroderma pigmentosum group A protein triggers DNA excision repair, *Nat. Struct. Mol. Biol. 13*, 278–284.
26. Shuck, S. C., Short, E. A., and Turchi, J. J. (2008) Eukaryotic nucleotide excision repair: from understanding mechanisms to influencing biology, *Cell Res. 18*, 64–72.

27. Aboussekhra, A., Biggerstaff, M., Shivji, M. K., Vilpo, J. A., Moncollin, V., Podust, V. N., Protic, M., Hubscher, U., Egly, J. M., and Wood, R. D. (1995) Mammalian DNA nucleotide excision repair reconstituted with purified protein components, *Cell 80*, 859–868.
28. Hermanson, I. L., and Turchi, J. J. (2000) Overexpression and purification of human XPA using a Baculovirus expression system, *Protein Expression Purif. 19*, 1–11.
29. Patrick, S. M., and Turchi, J. J. (2002) Xeroderma pigmentosum complementation group A protein (XPA) modulates RPA-DNA interactions via enhanced complex stability and inhibition of strand separation activity, *J. Biol. Chem. 277*, 16096–16101.
30. Neher, T. M., Rechkunova, N. I., Lavrik, O. I., and Turchi, J. J. (2010) Photo-cross-linking of XPC-Rad23B to cisplatin-damaged DNA reveals contacts with both strands of the DNA duplex and spans the DNA adduct, *Biochemistry 49*, 669–678.
31. Coan, K. E., Maltby, D. A., Burlingame, A. L., and Shoichet, B. K. (2009) Promiscuous aggregate-based inhibitors promote enzyme unfolding, *J. Med. Chem. 52*, 2067–2075.
32. Coan, K. E., and Shoichet, B. K. (2008) Stoichiometry and physical chemistry of promiscuous aggregate-based inhibitors, *J. Am. Chem. Soc. 130*, 9606–9612.
33. Jadhav, A., Ferreira, R. S., Klumpp, C., Mott, B. T., Austin, C. P., Inglese, J., Thomas, C. J., Maloney, D. J., Shoichet, B. K., and Simeonov, A. (2010) Quantitative analyses of aggregation, autofluorescence, and reactivity artifacts in a screen for inhibitors of a thiol protease, *J. Med. Chem. 53*, 37–51.
34. Feng, B. Y., and Shoichet, B. K. (2006) A detergent-based assay for the detection of promiscuous inhibitors, *Nat. Protoc. 1*, 550–553.
35. Walker, J. R., Corpina, R. A., and Goldberg, J. (2001) Structure of the Ku heterodimer bound to DNA and its implications for double-strand break repair, *Nature 412*, 607–614.
36. Glass, L. S., Bapat, A., Kelley, M. R., Georgiadis, M. M., and Long, E. C. (2010) Semi-automated high-throughput fluorescent intercalator displacement-based discovery of cytotoxic DNA binding agents from a large compound library, *Bioorg. Med. Chem. Lett. 20*, 1685–1688.
37. Alberts, B. (2009) Redefining cancer research, *Science 325*, 1319.
38. Helleday, T. (2010) Homologous recombination in cancer development, treatment and development of drug resistance, *Carcinogenesis 31*, 955–960.
39. Ikegami, T., Kuraoka, I., Saijo, M., Kodo, N., Kyogoku, Y., Morikawa, K., Tanaka, K., and Shirakawa, M. (1998) Solution structure of the DNA- and RPA-binding domain of the human repair factor XPA, *Nat. Struct. Biol. 5*, 701–706.
40. Buchko, G. W., Daughdrill, G. W., de, L. R., Rao, B. K., Isern, N. G., Lingbeck, J. M., Taylor, J. S., Wold, M. S., Gochin, M., Spicer, L. D., Lowry, D. F., and Kennedy, M. A. (1999) Interactions of human nucleotide excision repair protein XPA with DNA and RPA70 Delta C327: chemical shift mapping and 15N NMR relaxation studies, *Biochemistry 38*, 15116–15128.
41. Pettersen, E. F., Goddard, T. D., Huang, C. C., Couch, G. S., Greenblatt, D. M., Meng, E. C., and Ferrin, T. E. (2004) UCSF Chimera—a visualization system for exploratory research and analysis, *J. Comput. Chem. 25*, 1605–1612.
42. Lang, P. T., Brozell, S. R., Mukherjee, S., Pettersen, E. F., Meng, E. C., Thomas, V., Rizzo, R. C., Case, D. A., James, T. L., and Kuntz, I. D. (2009) DOCK 6: combining techniques to model RNA-small molecule complexes, *RNA 15*, 1219–1230.
43. Meng, E. C., Shoichet, B. K., and Kuntz, I. D. (1992) Automated docking with grid-based energy evaluation, *J. Comput. Chem. 13*, 505–524.
44. Graves, A. P., Shivakumar, D. M., Boyce, S. E., Jacobson, M. P., Case, D. A., and Shoichet, B. K. (2008) Rescoring docking hit lists for model cavity sites: predictions and experimental testing, *J. Mol. Biol. 377*, 914–934.